Numerical Solutions of Chaotic Convection Model in a Horizontal Layer of Fluid Using Deep Learning DNN

Ruwaidiah Idris[1*], Maharani Abu Bakar[2], Azwani Alias[3]

[1,2,3] Faculty of Ocean Engineering Technology and Informatics, Universiti Malaysia Terengganu, 21030 Kuala Nerus, Terengganu, Malaysia

*Corresponding author: ruwaidiah@umt.edu.my

ABSTRACT

In the subject of engineering, chaotic convection serves a critical function, for instance, magneto-mechanical devices, lasers, and mechanical and designing electrical circuits, as well as understanding fluid dynamics and oscillatory chemical reactions. Nonlinear chaotic systems, for instance, turbulence and fluid convection, exist up to modest external forcing levels before becoming unstable due to their extreme sensitivity to initial conditions. An uncontrolled system of convection will route the systems to unstable. When systems are unstable, it will damage the final product produced by industry such as microchips, crystal growth, welding of pipes line, etc. This paper developed a mathematical model for chaos convection in a fluid's horizontal layer derived using Galerkin truncated approximation techniques. Then, the obtained model was solved numerically using a multistep-deep learning neural network (DNN). We compared the results obtained graphically using multistep-DNN with the existing methods such as the Runge-Kutta method (RK), Euler method, and Livermore Solver for Ordinary Differential Equations (LSODE) method. It is found that multistep-DNN is able to solve the model efficiently and recover the results obtained using the RK method and LSODE method. However, for the Euler method, the results only cover small values of the Rayleigh number.

Keywords: Rayleigh-Bénard convection, chaotic convection, convective heat transfer, Galerkin techniques, multistep-DNN

1   INTRODUCTION

Convection problems are crucial in the establishment of fresh concepts about the relationship between chaos and order in flows, as well as between complexity and simplicity in the hydrodynamic object's behaviour and structure. Convective flows may generate greater or fewer ordered spatial structures. Studying them adds significantly to grasping the fundamental features of pattern-forming systems, which are the main topic of research in a synergetic, dynamic field of modern science. Rayleigh-Bénard convection, or convection in a plane horizontal fluid layer heated from below, is the most common kind of convection. Since there are no powerful streams driven by external conditions, temporal and spatial effects are generally decoupled in this occurrence.

For example, [8] explored a 2D fluid cell heated below as well as cooled from above, also known as the Rayleigh-Bénard problem. In an attempt to explain unexpected weather behaviour, the path to chaos in a fluid layer was intensively researched. The author then developed the model of fluid

convection, a 3D partial differential equations set. However, the author claimed that it is impossible to achieve acceptable precision in extremely long-range prediction since this model leads to chaotic behaviour [3]. Moreover, [5] looked at the issue of chaotic convection in porous media when the temperature was changed. They discovered that changing the temperature of the borders improves the chaotic motion's behaviour. Furthermore, [1] examined chaotic convection in a porous viscoelastic fluid saturated medium added with a heat source. Relying on the flow characteristics, the asymptotic behaviour might be chaotic, periodic, or stationary. In the meantime, [6] explores nonlinear thermal instability in a fluid layer. Moreover, the authors addressed how throughflow and gravity modulation, instead of the Rayleigh number, may be utilised to manage the chaos in the medium. Apart from that, [15] investigated the chaotic convection in a couple of stress fluid-saturated porous mediums under the condition of gravity modulation employing the chaotic Darcy-Brinkman model. The chaotic behaviour is linked to the significance threshold of the Rayleigh number that relies on the oscillation frequency as well as the Darcy-Brinkman couple stress factor, according to their findings.

The impact of gravity modulation, as well as rotation on chaotic convection, was studied by [7]. The author came to the conclusion that the Taylor number values and the g-jitter parameter affect the transformation from steady convection to chaos. In addition, [11] investigated chaotic convection in a ferrofluid added with internal heat production. They discovered that increasing the internal heat production hastens the system's instability. Moreover, raising the magnetic number to $M_1 = 2.5$ causes homoclinic bifurcation, which increases the convection process. Also, [4] delved into the investigation of chaotic and regular Rayleigh-Bénard convective movements in water and methanol. They revealed that in the instance of methanol, the thresholds for the commencement of chaotic and regular movements are lower than in water. Their findings also suggest that a growing zone for chaos exists before it becomes completely formed.

Apart from that, [12] modified the Vadasz-Lorenz model to examine phase-lag influences on the commencement of Darcy-Bénard chaotic and regular convection in a porous medium. It is discovered that the lag effect causes a numeric difference in the two chaos measurements and a qualitative variation in the character of chaos. Meanwhile, [9] investigated turbulent Rayleigh-Bénard convection within a cylinder in three dimensions. To derive the distinctive modes of turbulent thermal convection, the researchers employed the Propers Orthogonal Decomposition (POD) approach. Concurrently, in Rayleigh-Bénard convection, [14] investigated the persistence of large-scale circulation. The author comes to the conclusion that Rayleigh-Bénard convection behaviour varies with the Rayleigh number and occurs when Rayleigh number approaches transition levels between hard turbulence regimes, soft turbulence, transition, chaotic, convection, as well as conduction. By including extra higher-order harmonics in the spectral expansion of periodic solutions, [10] studied the systematic comparison that exists between the extended Lorenz equations as well as a direct numerical simulation in the 2D Rayleigh-Bénard convection.

Through the author's knowledge, most of the research that studied chaotic convection behaviour is solved conventionally. A system of differential equations (SDE) is explained numerically through the discretisation process to obtain the algebraic systems and thus solve it using the classical methods such as RK and Euler methods. Recently, deep learning technology has been developed to solve such SDE problems without the discretisation process, potentially making deep scientific learning a new sub-field of research. One popular method under machine learning, called multistep deep learning neural networks (DNN), is developed for solving the SDEs. The benefit of DNN used in this study is it can be combined with any optimiser methods to speed up the convergence. Therefore, the goal of

this work is to utilise DNN to analyse and resolve chaotic behaviour in a horizontal layer of fluid and compare the findings with those acquired by employing other methods.

2   MATHEMATICAL FORMULATION

Let a horizontal fluid layer with depth d between two parallel infinite stress-free boundaries. The fluid is heated below as well as cooled from above. Note that x-axis is measured along a lower boundary. Meanwhile, z-axis is measured vertically upwards. Furthermore, the lower surface adheres at the temperature T_0 meanwhile the upper surface is at $T_0 + \Delta T$, in which ΔT resembles the temperature difference between upper and lower surfaces.

The Boussinesq approximation is implemented to determine the impacts of density variations in the gravity term only. Here, the momentum equation is denoted as

$$\rho = \rho_0[1 - \beta(T - T_0)],$$

 in which β resembles the thermal expansion coefficient. Thus, the sets of non-dimensional equations commanding the motion of an incompressible fluid are expressed as follows

$$\frac{1}{Pr}\frac{\partial}{\partial t}\left(\frac{\partial u}{\partial z} - \frac{\partial w}{\partial x}\right) - \left(\frac{\partial}{\partial z}\frac{\partial^2 u}{\partial x^2} - \frac{\partial}{\partial x}\frac{\partial^2 w}{\partial z^2}\right) = Ra\frac{\partial T}{\partial x}, \tag{1}$$

$$\frac{\partial T}{\partial t} + u\frac{\partial T}{\partial x} + w\frac{\partial T}{\partial z} = \frac{\partial^2 T}{\partial x^2} + \frac{\partial^2 T}{\partial z^2}, \tag{2}$$

where T is the temperature, u, w denote the component of velocity in x and z-directions respectively, Pr is Prandtl number, where Ra denotes Rayleigh numbers. By incorporating the stream function specified by $u = \partial\psi/\partial z$ as well as $w = -\frac{\partial\psi}{\partial x}$, we have:

$$\left[\left(\frac{1}{Pr}\frac{\partial}{\partial t} + \left(\frac{\partial^2\psi}{\partial x^2} + \frac{\partial^2\psi}{\partial z^2}\right)\right)\right]\left(\frac{\partial^2\psi}{\partial x^2} + \frac{\partial^2\psi}{\partial z^2}\right) = -Ra\frac{\partial T}{\partial x}, \tag{3}$$

$$\frac{\partial T}{\partial t} - \left(\frac{\partial^2 T}{\partial x^2} + \frac{\partial^2 T}{\partial z^2}\right) = \frac{\partial\psi}{\partial x}\frac{\partial T}{\partial z} - \frac{\partial\psi}{\partial z}\frac{\partial T}{\partial x}. \tag{4}$$

Provided that the boundaries are isothermal and stress-free, hence the boundary conditions are expressed as follows

$$w = \frac{\partial^2 w}{\partial z^2} = T = 0 \quad at \quad z = 0 \quad and \quad z = 1. \tag{5}$$

The nonlinear couple of systems formed by Eqns. (3) and (4), along with the related boundary conditions, provide a fundamental stationary conduction solution. The Galerkin truncated approximation is subsequently employed to address these problems.

2.1   Diminished Set of Equation

In this section, we will discuss the solutions of Eqns. (3)–(4) for linear stability analysis and weakly nonlinear analysis.

2.1.1   Linear Stability Analysis

By examining simply the marginal stationary state, the principle of exchange of stabilities (PES) may be easily validated. We assume the linear and steady-state versions of Eqns. (3) and (4). Here, utilising periodic waves of the form [2] as the solution yields:

$$\psi = A_0 sin(a\pi x)sin(\pi z), \tag{6}$$

$$\theta = B_0 cos(a\pi x)sin(\pi z). \tag{7}$$

Here, A_0 and B_0 are the stream function and temperature values, respectively, while a is the horizontal wavenumber. We have the normal mode solutions of Eqns. (6) and (7) with the boundary conditions in Eqn. (5). The critical Rayleigh number may be expressed in the following way using the conventional process:

$$R_c = \frac{27\pi^2}{4}. \tag{8}$$

The critical Rayleigh number resembles the transition behaviour from nonlinear to linear instability.

2.1.2   Weakly Nonlinear Analysis

In order to gain the answer to Eqns. (3) and (4), we denote the stream function as well as temperature distribution in the following equations

$$\psi = A_1 \sin\left(\frac{\pi x}{L}\right)\sin(\pi z), \tag{9}$$

$$T = B_1 \cos\left(\frac{\pi x}{L}\right)\sin\pi z + B_2 \sin(2\pi z). \tag{10}$$

Substituting Eqns. (9) and (10) into Eqns. (3) and (4), multiplying the equations by the orthogonal eigenfunctions corresponding to Eqns. (9) and (10), as well as integrating these equations with respect to the spatial domain, gives a set of three ordinary differential equations (ODE) for the amplitudes time evolution given by:

$$\frac{dA_1}{d\tau} = -\frac{Pr\gamma}{\pi^2}\left[A_1 + \frac{Ra}{\theta\pi}B_1\right], \tag{11}$$

$$\frac{dB_1}{d\tau} = -B_1 - \frac{1}{\theta\pi}A_1 - \frac{1}{\theta}A_1B_2, \tag{12}$$

$$\frac{dB_2}{d\tau} = \frac{1}{2\theta}A_1B_1 - 4\gamma B_2. \tag{13}$$

From the equations mentioned above, time was rescaled, where additional notation was proposed:

$$\tau = \frac{(L^2+1)\pi^2 t}{L^2}, \quad \theta = \frac{(L^2+1)}{L}, \quad \gamma = \frac{L}{\theta} = \frac{L^2}{(L^2+1)}, \quad R = \frac{Ra}{\pi^2\theta^2} \quad and \quad \alpha = \frac{Pr\gamma}{\pi^2}. \tag{14}$$

It is apparent to establish the additional notation given by:

$$R = \frac{Ra}{\pi^2\theta^2}, \quad \alpha = \frac{Pr\gamma}{\pi^2}, \tag{15}$$

as well as to rescale the amplitudes in the equation of:

$$X = -\frac{A_1}{2\theta\sqrt{2\gamma}}, \quad Y = \frac{\pi R B_1}{2\sqrt{2\gamma}}, \quad and \quad Z = -\pi R B_2. \tag{16}$$

Then, we obtained the following possible set of systems

$$\dot{X} = \alpha(Y - X),$$

$$\dot{Y} = RX - Y - XZ, \tag{17}$$

$$\dot{Z} = XY - \gamma Z,$$

in which the dots (·) resemble time derivatives of d( )/dτ. Moreover, the system given in (17) equals to the Lorenz equations [8, 13].

3   RESULTS AND DISCUSSION

The system of (17) is addressed employing a multistep-DNN approach operating on Jupiter software under Google Collaboratory to characterise the dynamic behaviour of thermal convection in a horizontal fluid layer. Moreover, the values for α and γ utilized in all computation are 10 and 8/3, correspondingly, similar to those values considered by [8]. The common initial conditions used in this computation are $\tau = 0$: $X = Y = Z = 0.9$. All computations were performed with the maximum time value of $\tau_{max} = 250$ having the step size $\Delta\tau = 0.01$. Afterward, the outcomes acquired will be compared with the results obtained by [8] as shown in [13] using the Euler method, Runge-Kutta (RK) method, and Livermore Solver for Ordinary Differential Equations (LSODE) method.

Figures 1–7 depicts the projections of the trajectories' data on the $X - Y - Z$ plane solved using the Euler method by [13] as shown in (a), Runge-Kutta method in (b), LSODE in (c), and a new proposed method multistep-DNN as plotted in (d). In Figure 1, for $R = 1.5$, the Rayleigh number is a slight loss of the motionless solution stability. From the figures, we can detect that the findings are in good agreement between the four methods.
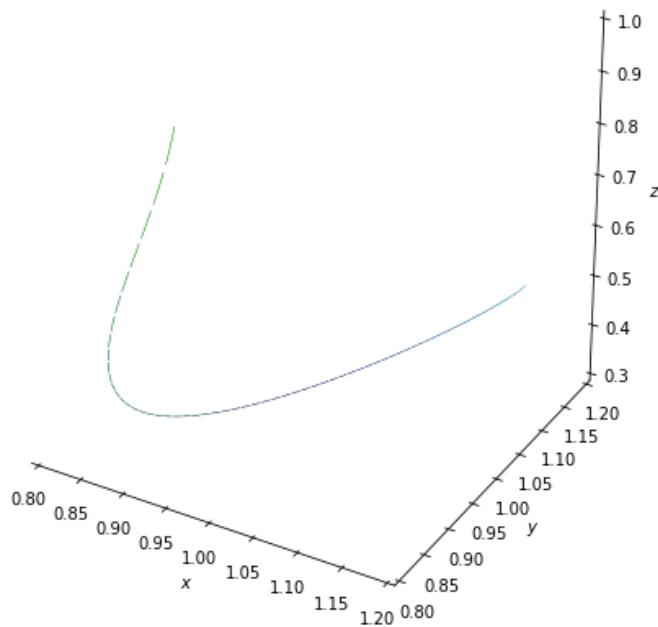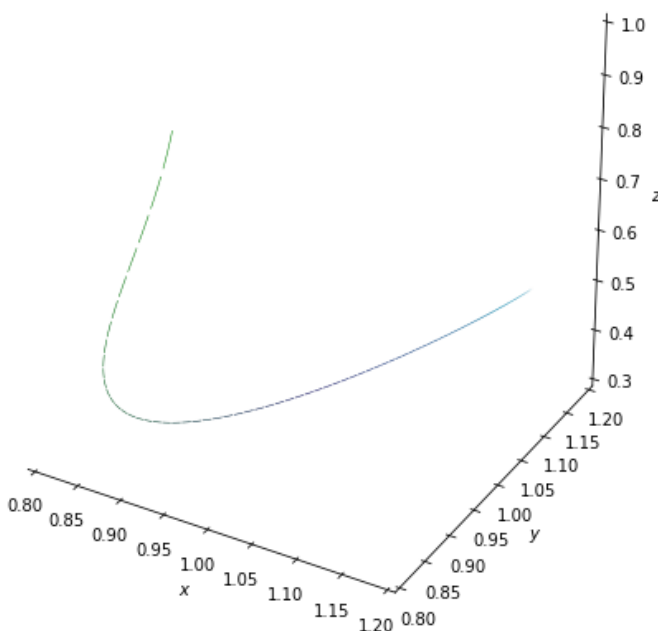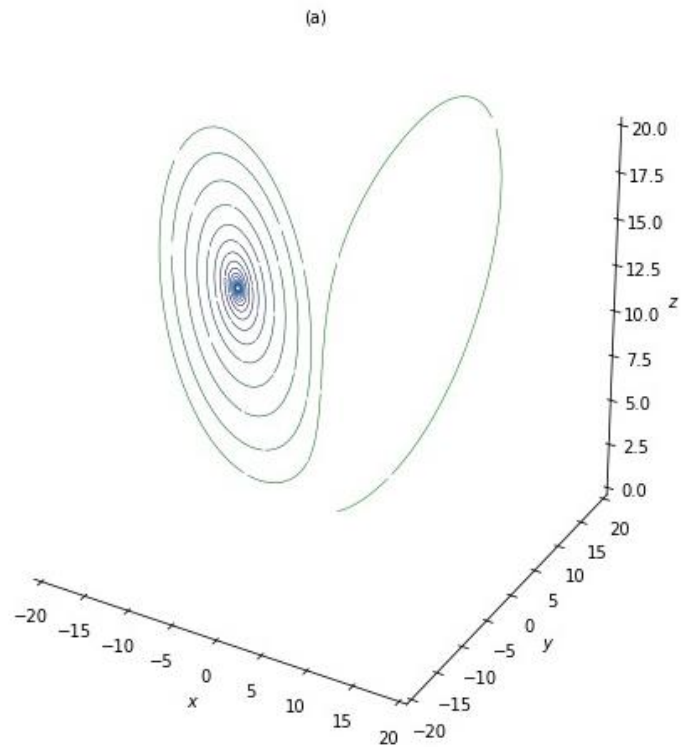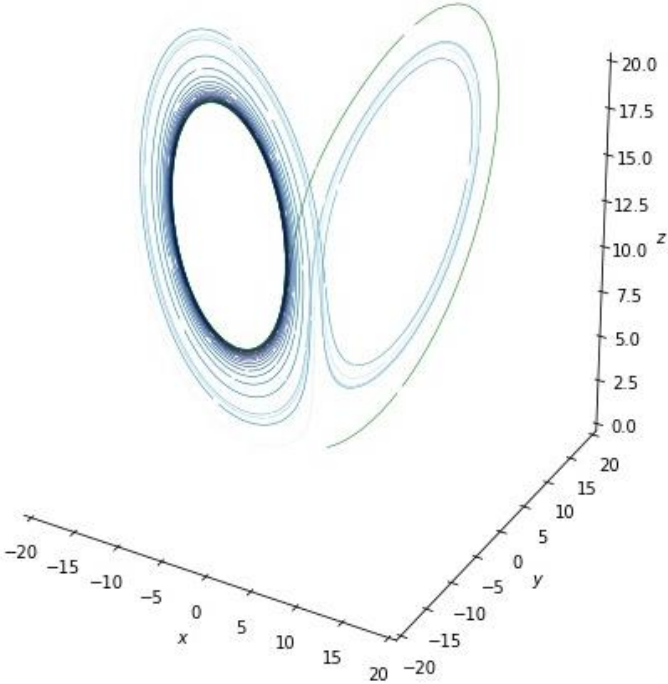
(a)
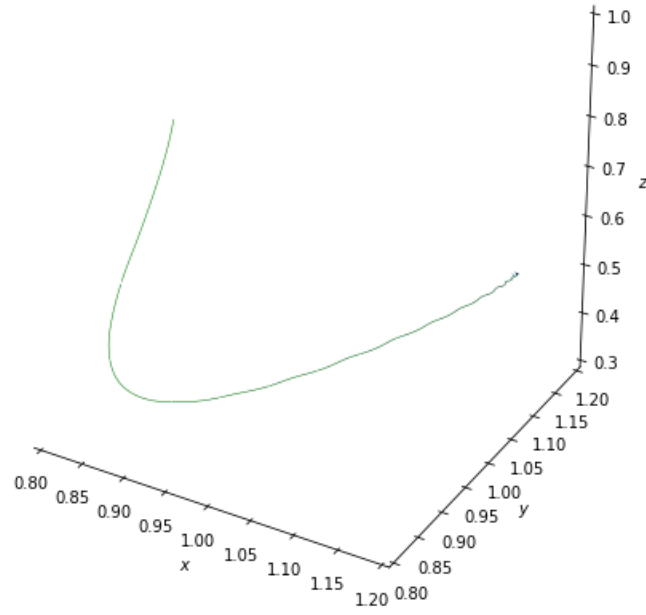
(b)
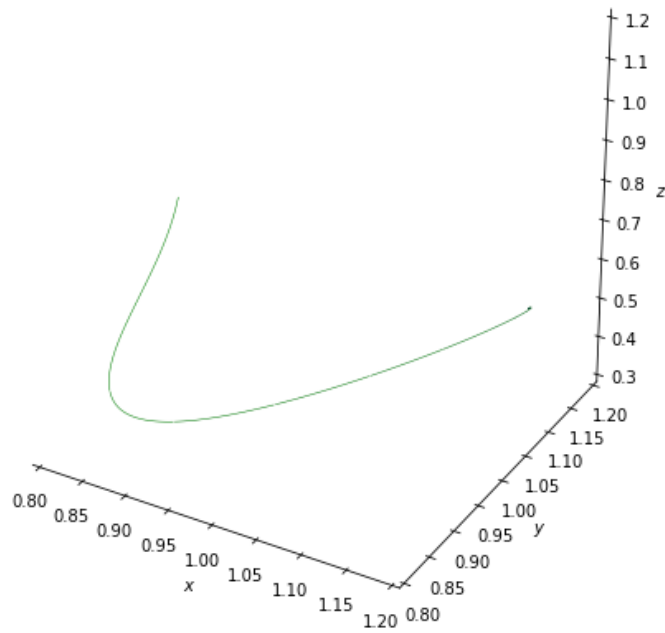
(c)

(d)

Figure 1: Phase portrait plot for $R = 1.5$, (a) Runge-Kutta method, (b) Euler method, (c) LSODE method, (d) multistep-DNN method

For $R = 15$, the spiralling approaches the fixed point, where the motion rate is increasing in the angular direction, as shown in Figures 2 (a), (c), and (d) but not in (b). Using the Euler method, (b), we can see that a white hole surrounding the convection fixed point illustrates that the maximum time distributed for the computation was inadequate for the trajectory to attain the fixed point. Similar behaviour also occurs for $R = 24.74$ using RK method, LSODE method, and multistep-DNN method, as shown in Figure 3.

(a)

(b)

(c)

(d)
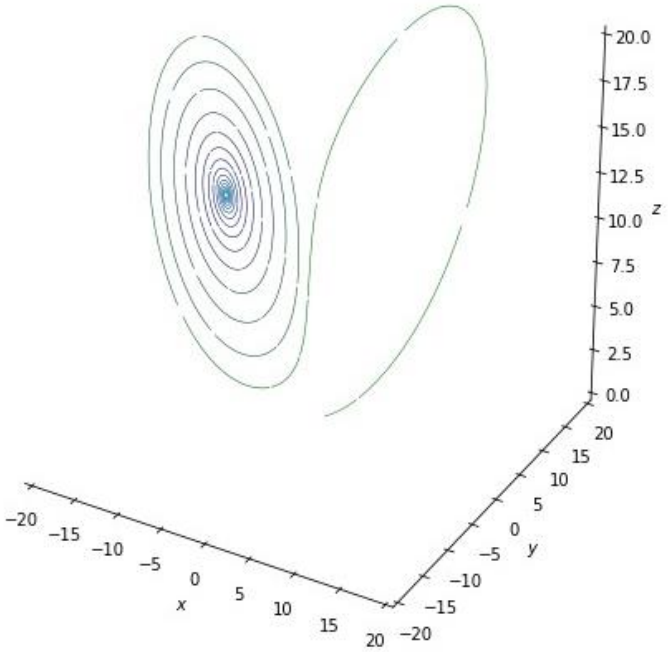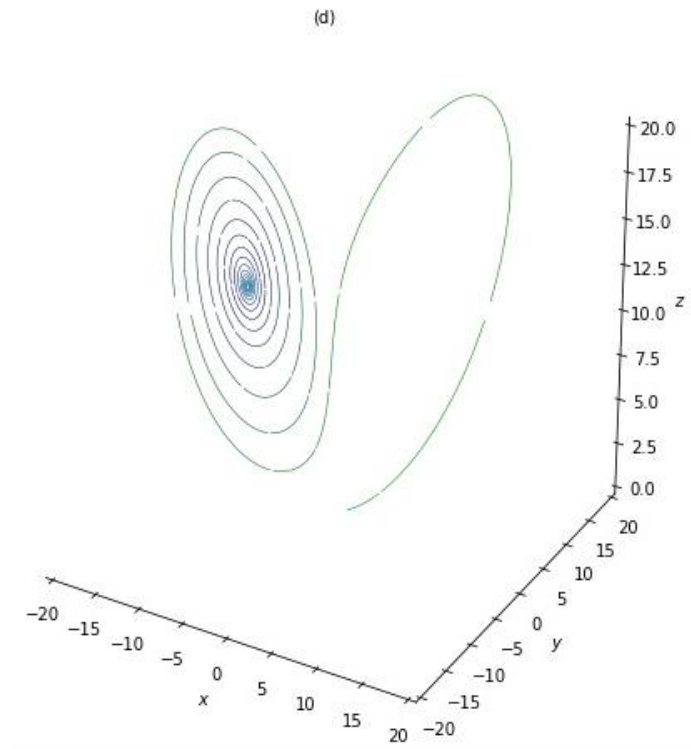
Figure 2: Phase portrait plot for $R = 15$, (a) Runge-Kutta method, (b) Euler method, (c) LSODE method, (d) multistep-DNN method
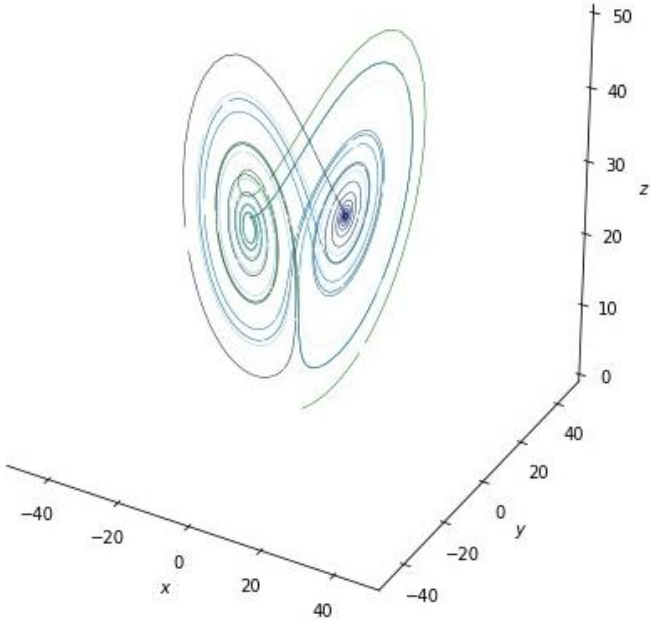
(a)
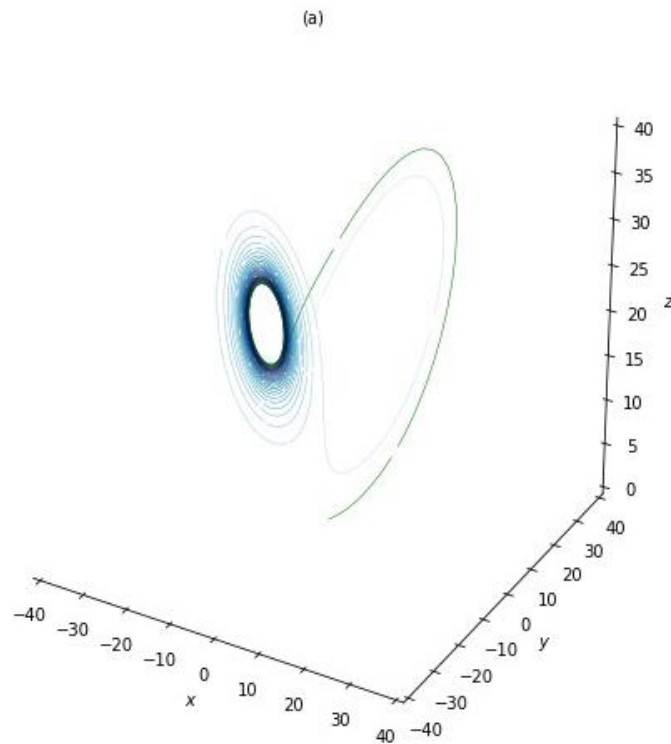
(b)
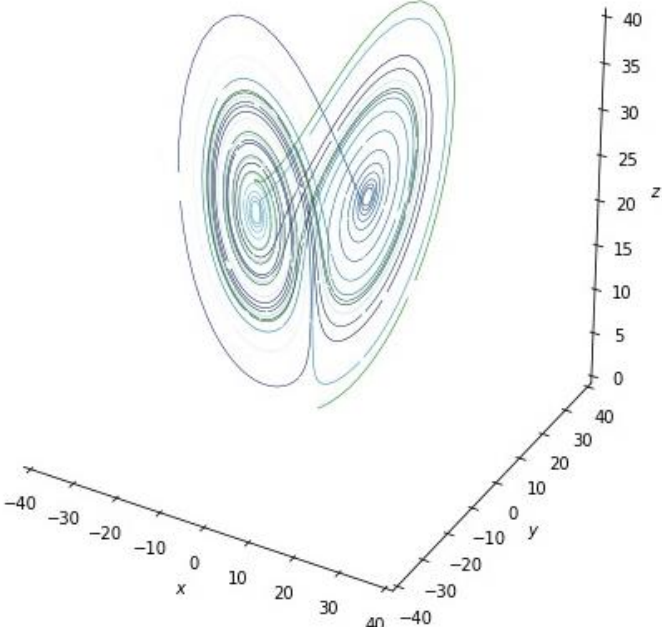
(c)
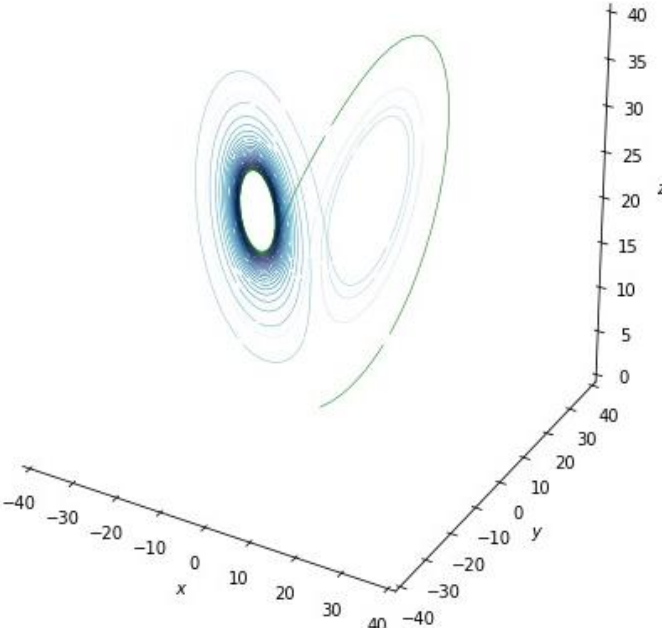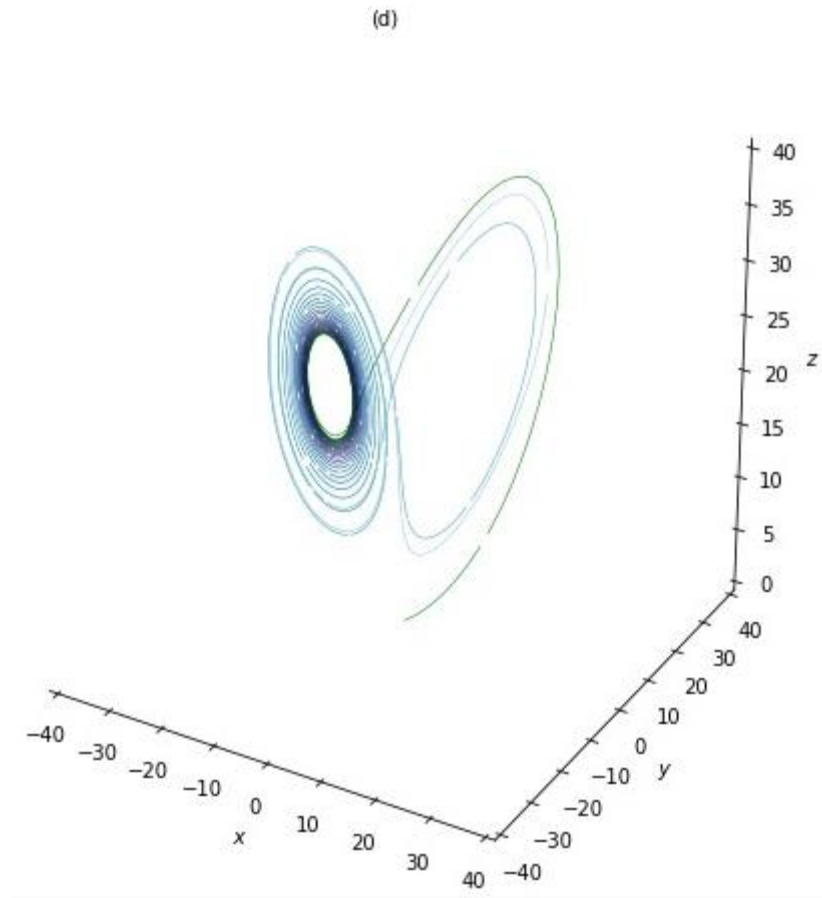
Figure 3: Phase portrait plot for $R = 24.74$, (a) Runge-Kutta method, (b) Euler method, (c) LSODE method, (d) multistep-DNN method

Meanwhile, Figure 4 shows the trajectories data point for $R = 28$. The findings exhibit that homoclinic explosion exists while chaotic regime with the strange attractor takes over utilising RK method (a), LSODE (c) method, and multistep-DNN method (d). Still, period 8 occurs using the Euler method (b).
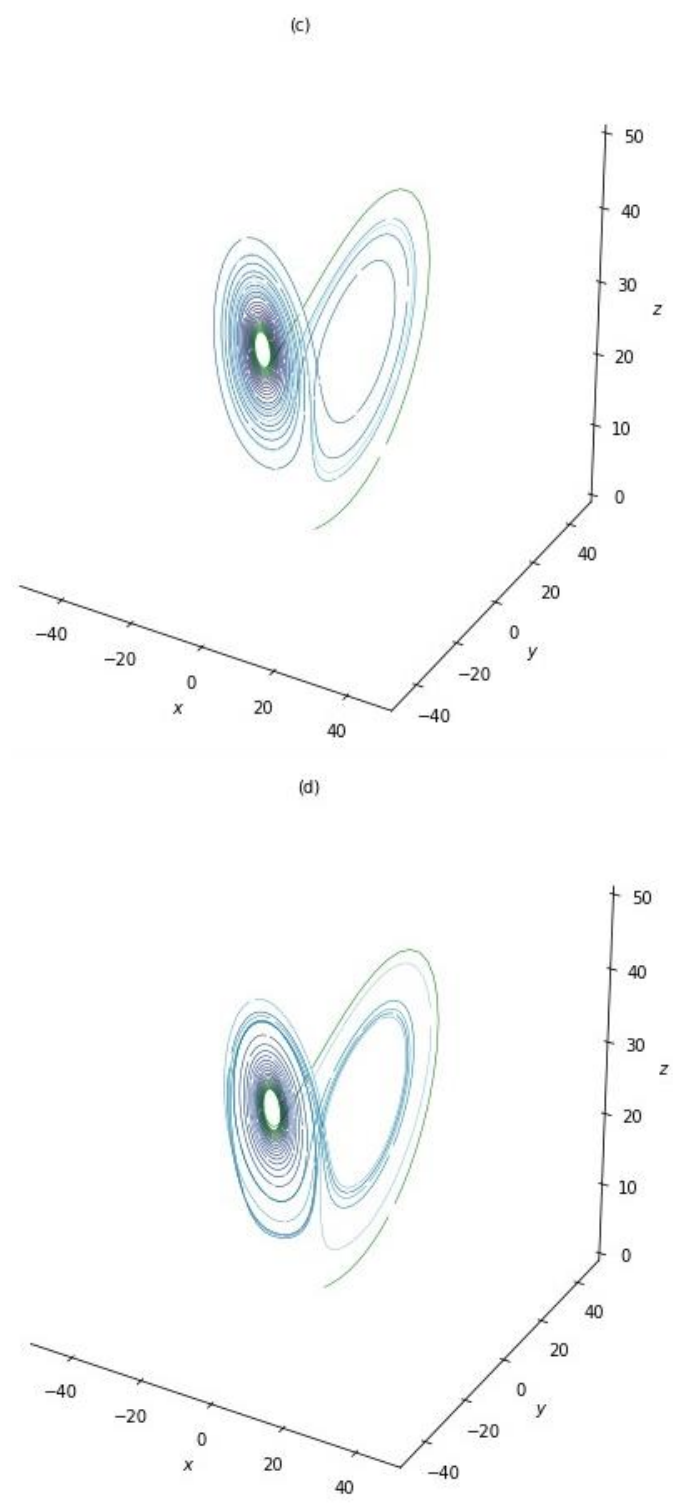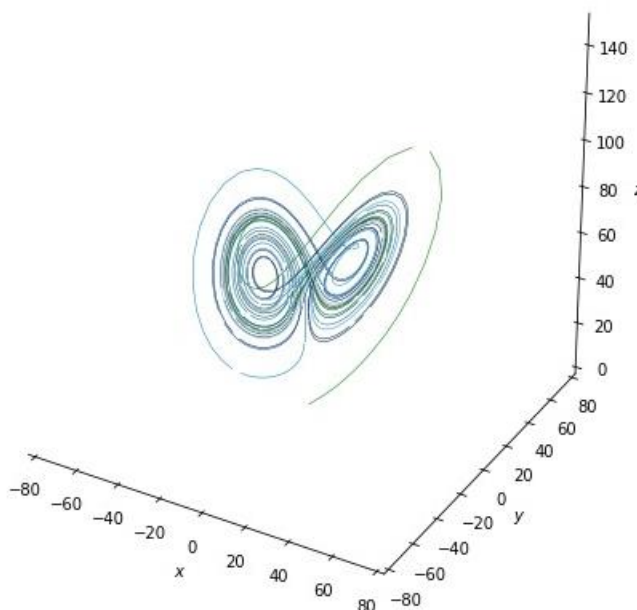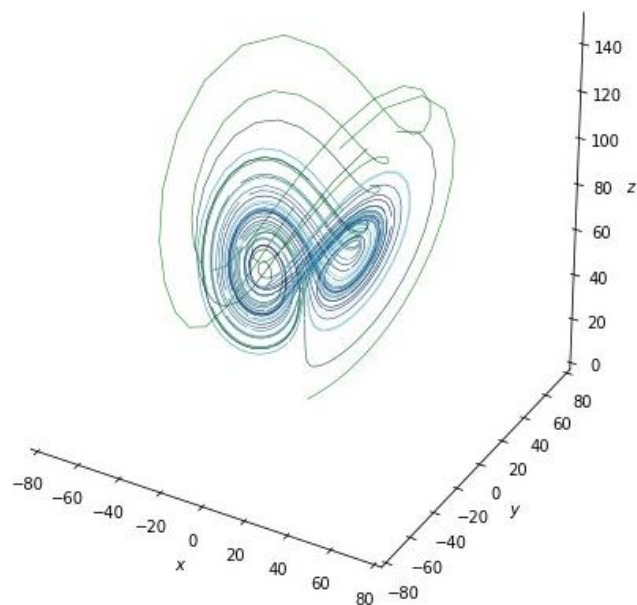
(a)

(b)

(c)

(d)
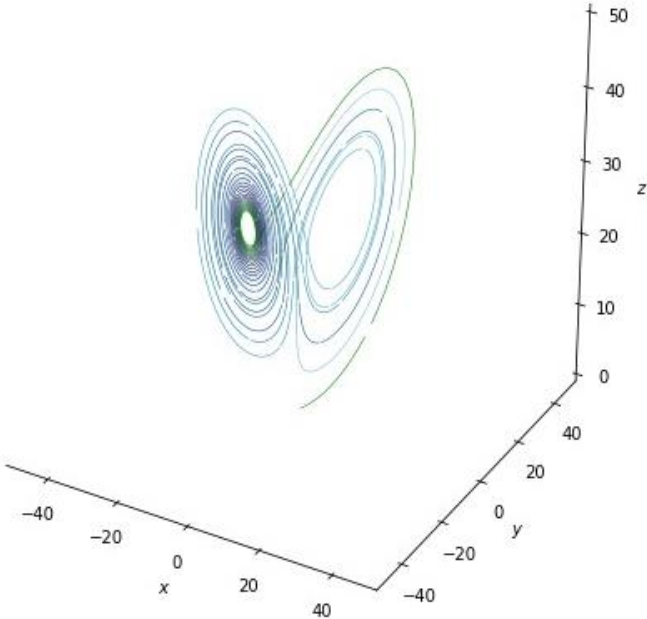
Figure 4: Phase portrait plot for $R = 28$, (a) Runge-Kutta method, (b) Euler method, (c) LSODE method, (d) multistep-DNN method

A homoclinic explosion to stable periodicity takes over for $R = 61.5$ as presented in Figure 5 (a), (c), and (d) using the RK method, LSODE method, and multistep-DNN method. Meanwhile, using the Euler method (d), we obtain the chaotic regime.
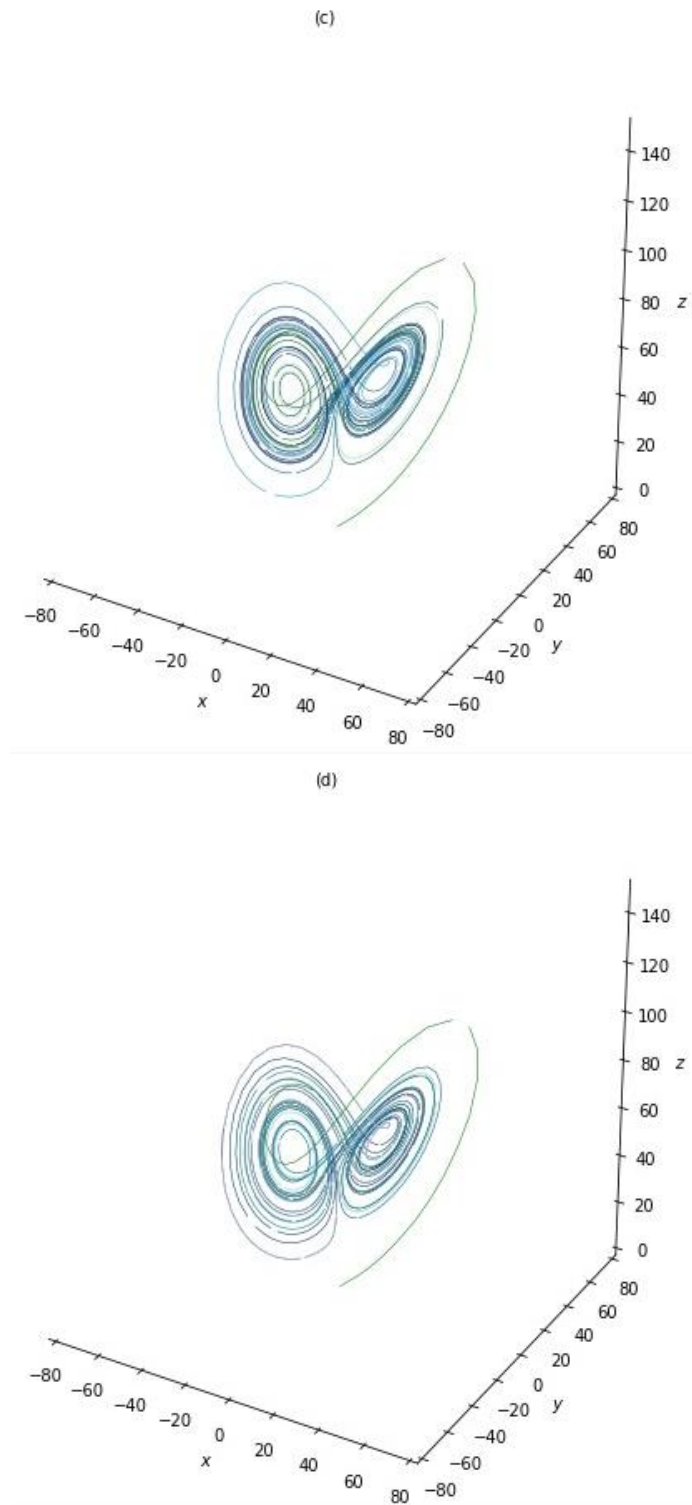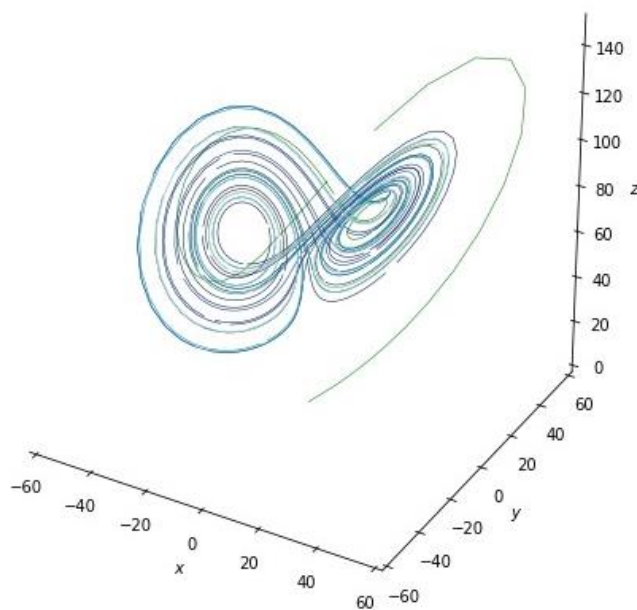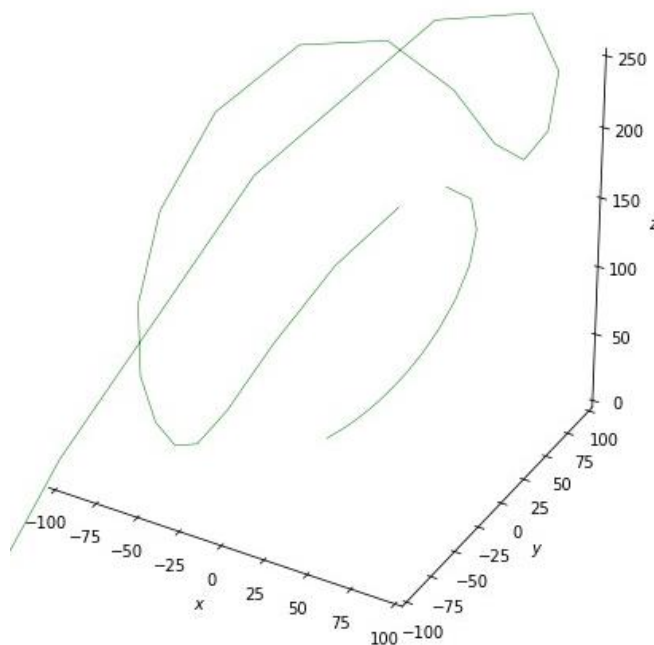
(a)

(b)

(c)

(d)

Figure 5: Phase portrait plot for $R = 61.5$, (a) Runge-Kutta method, (b) Euler method, (c) LSODE method, (d) multistep-DNN method

At $R = 80$, the chaotic regime takes over as shown in Figures 6 (a), (c), and (d). However, for Figure 6 (b), we cannot conclude any behaviour using the Euler method since this method is numerically unstable for many iterations.
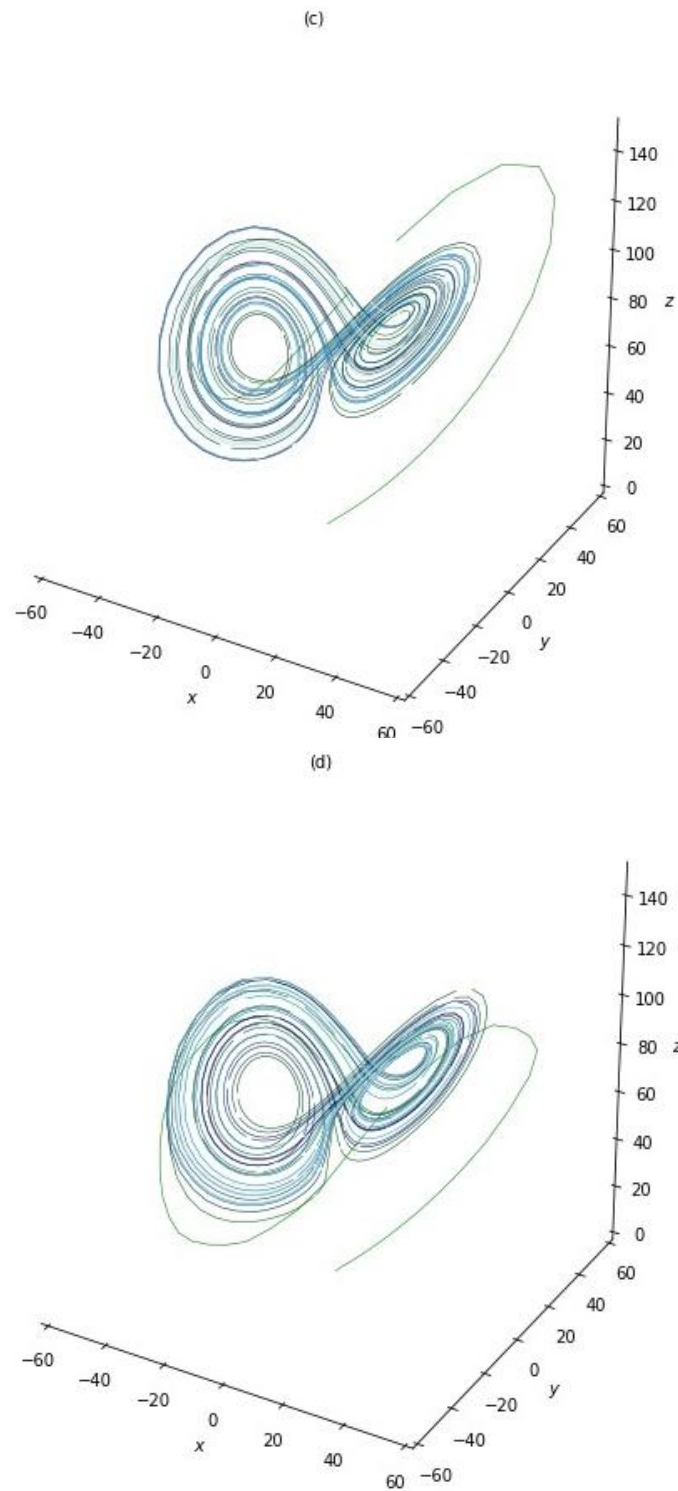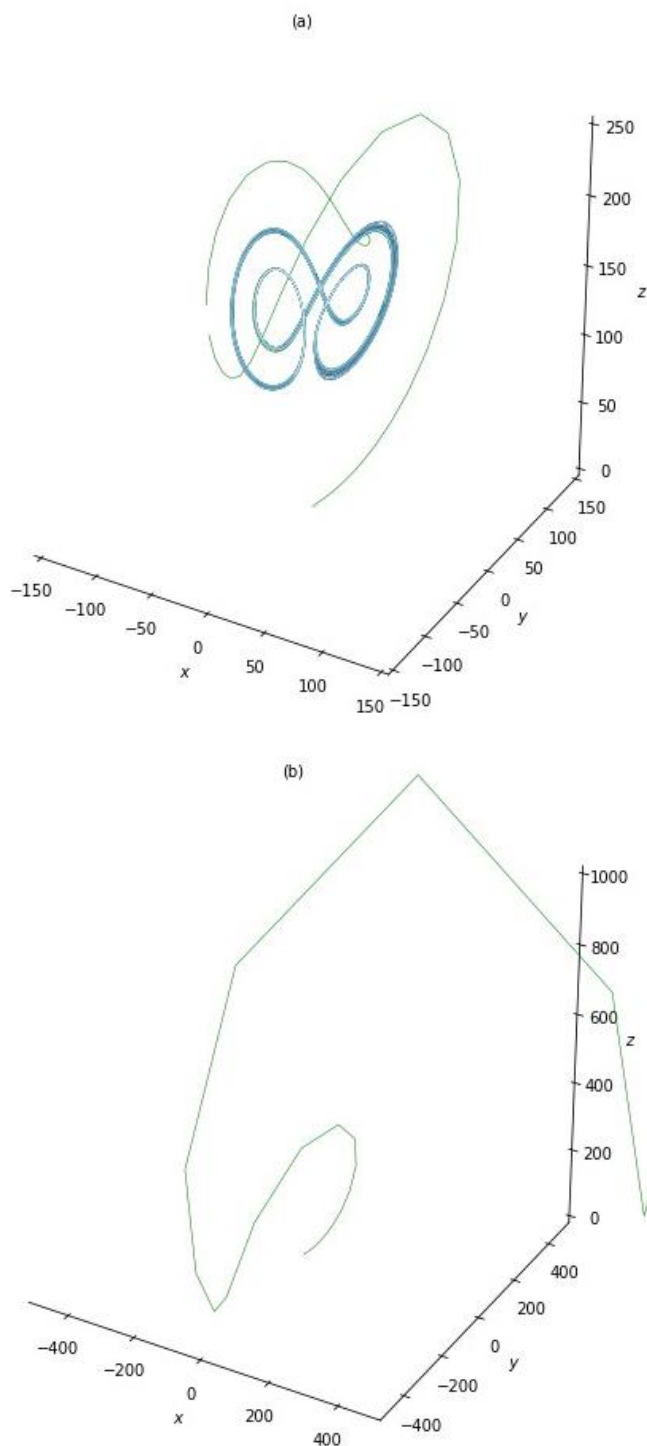
(a)

(b)

(c)

(d)

Figure 6: Phase portrait plot for $R = 80$, (a) Runge-Kutta method, (b) Euler method, (c) LSODE method, (d) multistep-DNN method

Figures 7 (a) and (c) display that period-2 periodic solution exists at $R = 147.5$. In Figure 7 (d), the system remains chaotic. These results occur due to convergence issues. Therefore, we need to improve the multistep-DNN method by considering other optimiser methods in order to speed up the convergence. Further studies are needed relating to these issues.
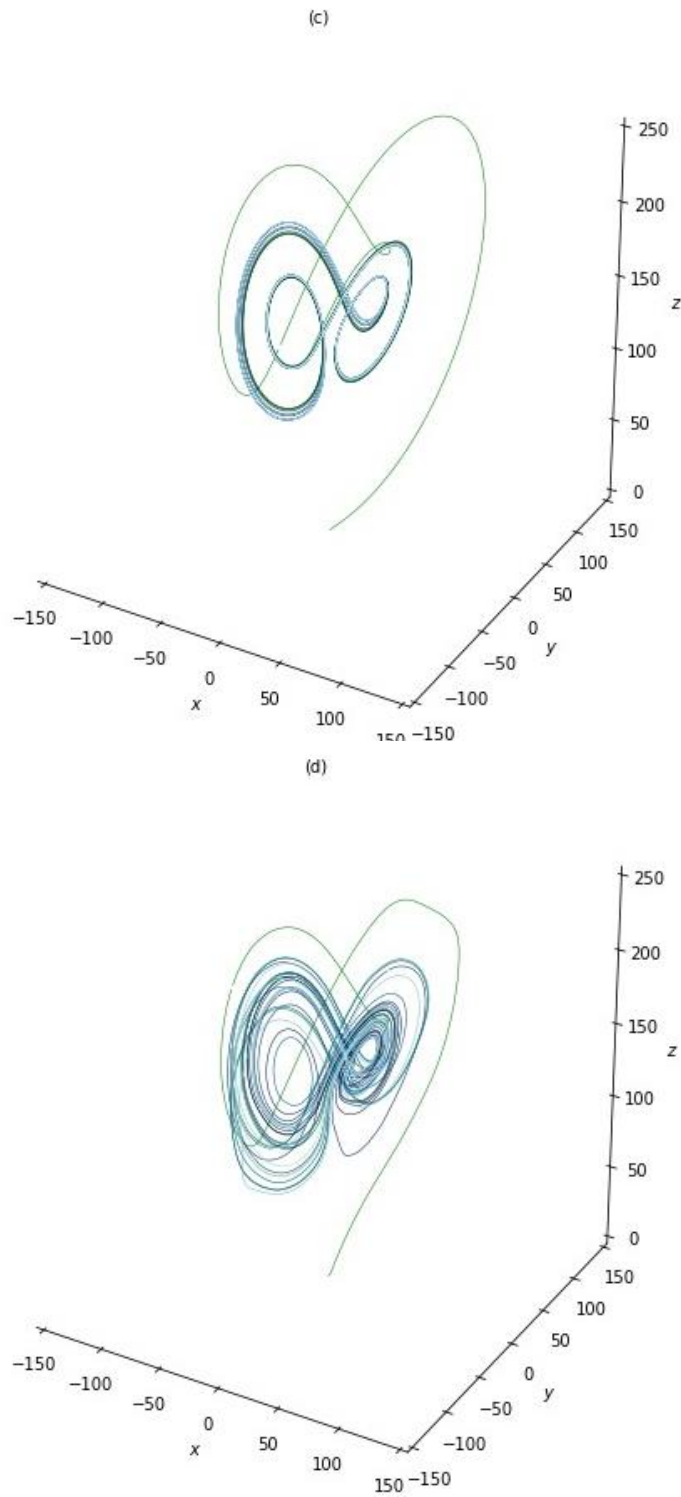
(a)

(b)

(c)

(d)

Figure 7: Phase portrait plot for $R = 147.5$, (a) Runge-Kutta method, (b) Euler method, (c) LSODE method, (d) multistep-DNN method

4   CONCLUSION

The chaotic behaviour of a horizontal layer of fluid was explored in this work, and the problem was solved utilising the multistep-DNN method. The results obtained are compared with the results using the RK method, Euler method, and LSODE method. At a slightly subcritical value of the Rayleigh number, the transition from steady convection to chaos occurs via a Hopf bifurcation connected with a homoclinic explosion. From the results obtained, we can conclude that the multistep-DNN is capable of solving the system of (17) similar to the RK method and LSODE method. However, further studies are needed to improve this method for large values of Rayleigh numbers. Furthermore, this limitation needs further investigation in order to produce good results to solve the dynamical systems of equations.

REFERENCES

[1]   B. S. Bhadauria, "Chaotic convection in a viscoelastic fluid saturated porous medium with a heat source," *Journal of Applied Mathematics*, vol. 2016, pp. 1–18, 2016.

[2]   S. Chandrasekhar, *Hydrodynamics and hydromagnetic stability*. Oxford: Oxford University, 1961.

[3]   Z.-M. Chen and W. G. Price, "On the relation between Rayleigh–Bénard convection and Lorenz System," *Chaos, Solitons & Fractals*, vol. 28, no. 2, pp. 571–578, 2006.

[4]   S. Kanchana, Y. Su, and Y. Zhao, "Regular and chaotic Rayleigh-Bénard convective motions in methanol and water," *Communications in Nonlinear Science and Numerical Simulation*, vol. 83(105129), pp. 1–20, 2020.

[5]   P. Kiran and B. S. Bhadauria, "Chaotic convection in a porous medium under temperature modulation," *Transport in Porous Media*, vol.107, pp. 745–763, 2015.

[6]   P. Kiran, K. Geethanjali, and Y. Narasimhulu, "Chaotic convection in the presence of throughflow," *International Journal of Pure and Applied Mathematics*, vol. 117, no. 11, pp. 357–367, 2017.

[7]   P. Kiran, *"G-Jitter Effects on Chaotic Convection in a Rotating Fluid Layer,"* in *Advances in Condensed-Matter and Materials Physics - Rudimentary Research to Topical Technology,* J. Thirumalai and S. I. Pokutnyi, Eds., IntechOpen, 2020.

[8]   E. N. Lorenz, "Deterministic nonperiodic flow," *Journal of Atmospheric Sciences*, vol. 20, pp. 130–141, 1963.

[9]   G. Paolillo, C. S. Greco, T. Astarita, and G. Cardone, "Experimental determintation of the 3-D characteristic modes of turbulent Rayleigh-Bénard convection in a cylinder," *Journal of Fluid Mechanics*, vol. 922, p. A35, 2021.

[10]   J. Park, S. Moon, J. M. Seo, and J. J. Baik, "Systematic comparison between the generalised Lorenz equations and DNS in the two-dimensional Rayleigh-Bénard convection," *Chaos: An Interdisciplinary Journal of Nonlinear Science*, vol. 31, p. 073119, 2021.

[11]   H. H. Senin, N. F. M. Mokhtar, and M. H. A. Sathar, "Chaotic convection in a ferrofluid with internal heat generation," *CFD Letters*, vol.12, no. 10, pp. 62–74, 2020.

[12]   P. G. Siddheshwar, C. Kanchana, and D. Laroze, "A study of Darcy-Bénard regular and chaotic convection using a new local thermal non-equilibrium formulation," *Physics of Fluids*, vol. 33, no. 4, p. 044107, 2021.

[13]   C. Sparrow, *The Lorenz equations: Bifurcations, Chaos and Strange Attractors*. New York: Springer-Verlag, 1982.

[14]   P. Wei, "The persistence of large-scale circulation in Rayleigh-Bénard convection," *Journal of Fluid Mechanics*, vol. 924, p. A28, 2021.

[15]   M. Zhao, S. Wang, S. C. Li, Q. Y. Zhang, and U. S. Mahabaleshwar, "Chaotic Darcy-Brinkman convection in a fluid saturated porous layer subjected to gravity modulation," *Results in Physics*, vol.9, pp. 1468–1480, 2018.